Plasmonic wave plate based on subwavelength nanoslits

Eng Huat Khoo,[1,2,3] Er Ping Li,[2] and Kenneth B. Crozier[1,4]

[1]*School of Engineering and Applied Science, Harvard University, Cambridge, Massachusetts 02138, USA*

[2]*Institute of High Performance Computing, A-STAR, 1 Fusionopolis Way, Connexis, Singapore 138632*

[3]*e-mail: khooeh@ihpc.a-star.edu.sg*

[4]*e-mail: kcrozier@seas.harvard.edu*

Received January 26, 2011; revised June 7, 2011; accepted June 8, 2011;
posted June 8, 2011 (Doc. ID 141519); published June 24, 2011

We propose a quarter-wave plate based on nanoslits and analyze it using a semianalytical theory and simulations. The device comprises two nanoslits arranged perpendicular to one another where the phases of the fields transmitted by the nanoslits differ by $\lambda/4$. In this way, the polarization state of the incident light can be changed from linear to circular or vice versa. The plasmonic nanoslit wave plate is thin and has a subwavelength lateral extent. We show that the predictions for the phase shift obtained from a semianalytical model are in very good agreement with simulations by the finite difference time domain method. © 2011 Optical Society of America

OCIS codes: 250.5403, 240.5420, 310.6628, 260.5430.

The phenomenon of extraordinary optical transmission has been studied extensively in nanoholes [1] and nanoslits [2,3], mainly because it addresses the long-standing problem of the low transmission of light through subwavelength apertures [4]. In addition to investigating boosting the transmission efficiency of nanoslits, the phase shift upon transmission has also been discussed. The amplitude and phase of the fields transmitted by nanoslits are sensitive to their dimensions (i.e., length, width, and metal film thickness) [5,6]. The transmission phase shift can also be modified by filling the nanoslit with a dielectric or by using two layers of slits [7]. Planar lenses have been demonstrated using a group of several nanoslits with an engineered phase shift [8]. The ability of nanoslits to modify phase in a precise manner suggests that they may also be useful for polarization control.

In this Letter, a plasmonic wave plate based on nanoslits is proposed for the first time to the best of our knowledge. Plasmonic wave plates have been previously demonstrated using a single circular aperture surrounded by an elliptical antenna grating [9]. In that design, the path length difference between the long and short axes of the elliptical grating generated a phase shift of $\lambda_{sp}/4$ for light polarized along these axes. In the device we propose, the wave plate instead comprises nanoslits, which are arranged to provide the phase shift between the polarization components of the incident light along their axes. The phase shift is tailored by making each slit in the pair have different lengths and widths. We also consider the case where one nanoslit is filled with glass [10] while the other is unfilled to increase the phase difference.

The plasmonic wave plate consists of a gold film of thickness $t = 200\,\text{nm}$ deposited on a glass substrate. Two nanoslits placed perpendicular to each other are formed in the gold film, as shown in Fig. 1(a). Here, we consider an isolated pair of nanoslits. This is done by simulating a $3\,\mu\text{m} \times 3\,\mu\text{m}$ square region with a nanoslit pair in the center, with perfectly matched layer boundary conditions at the x, y, and z boundaries. The simulations are performed using the finite difference time domain (FDTD) method. A linearly polarized plane wave, with its electric field vector at 45° from the x- and y-axes, is normally incident from the glass side. The nanoslits parallel to the x- and y-axes are labeled N_x and N_y, respectively. For the structure of Fig. 1(a), the slits N_x and N_y are identical, having lengths of $l = 420\,\text{nm}$ and widths of $w = 40\,\text{nm}$. The transmission is found by monitoring the signal at a $3\,\mu\text{m} \times 3\,\mu\text{m}$ detection screen on the air side, at a distance of $5\,\mu\text{m}$ from the metal–air interface.

In Fig. 1(b), we consider the cases for which the nanoslits are unfilled and filled with glass, whose index is taken to be 1.47. This is also the index for the substrate. The normalized-to-area transmission is the transmitted power normalized to the product of the area of the nanoslit openings with the illumination intensity. It can be seen that there is a resonance from the nanoslit cavity at a wavelength of 802 nm for the unfilled case, but this redshifts to 954 nm in the glass-filled case. The phase of the z component of the electric field (E_z) transmitted

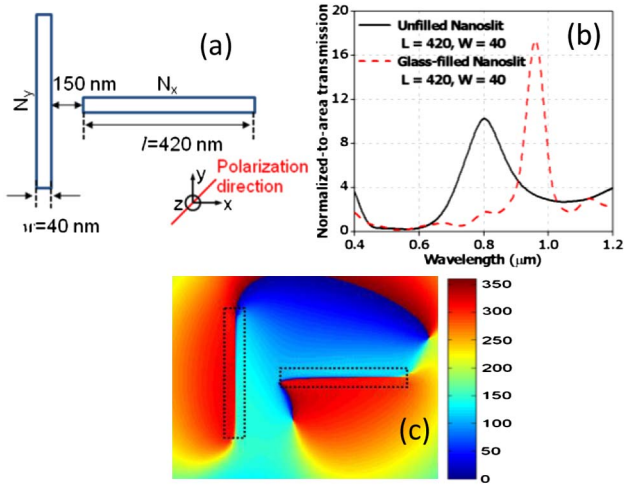

Fig. 1. (Color online) (a) Schematic layout of device comprising nanoslits with identical dimensions oriented perpendicular to one another. (b) Transmission spectra of a pair of unfilled and filled nanoslits. The glass-filled nanoslit pair exhibits a transmission resonance that is redshifted from that of the unfilled nanoslit pair. (c) Phase of E_z transmitted through unfilled nanoslits at metal–air interface.

through the unfilled nanoslits at the metal–air interface is shown in Fig. 1(c) at a free space wavelength of $\lambda = 802\,\text{nm}$. From Fig. 1(c), it can be seen that the E_z fields at the exits of N_x and N_y have identical phases. The E_z phase in N_x (N_y) shows a π phase difference on the upper and lower part (left and right part) of the nanoslit, consistent with the fundamental odd-mode of a metal–insulator–metal (MIM) waveguide excited in the E_y (E_x) direction.

We now consider how to achieve a phase difference upon transmission between the x- and y-polarized components of the electric field. We modify the nanoslit N_x to make its transmission exhibit a phase delay with respect to that of N_y. It was reported that by changing the width of the nanoslit [11], the phase of the light exiting can be modified. The nanoslits can be modeled as MIM heterostructures. The propagation constant of these MIM structures increases as the slit width decreases [8] and is determined from the MIM dispersion relation [12,13]

$$\tanh\left(\frac{w}{2}\sqrt{\beta^2 - \varepsilon_1 k_0^2}\right) = \frac{-\varepsilon_1\sqrt{\beta^2 - \varepsilon_m k_0^2}}{\varepsilon_m\sqrt{\beta^2 - \varepsilon_1 k_0^2}}, \qquad (1)$$

where ε_1 and ε_m are the permittivities of the material in the nanoslit and surrounding metal, respectively. The variable β is the propagation constant in the nanoslit and k_0 is the incident wave vector. However, we need to take into account the fact that the nanoslit has finite length. This yields an effective propagation constant of [14]

$$\beta_{\text{eff}} = \sqrt{\beta^2 - \left(\frac{\pi}{l}\right)^2}. \qquad (2)$$

The phase of the light passing through the nanoslit is given by $\beta_{\text{eff}} \times t$ [5]. Other additional phase terms such as additional phase change from the nanoslit resonance are neglected because the term $\beta_{\text{eff}} \times t$ plays the dominant role [6]. One effective means for increasing the phase difference is to fill one of the nanoslits with a high index material. As shown in Fig. 1(b), however, this redshifts the transmission resonance. To mitigate this, we match the resonance wavelengths by modifying the widths and lengths of N_x and N_y, as shown in Fig. 2(a). The modified glass-filled nanoslit N_x has length $l_x = 292\,\text{nm}$ and width $w_x = 40\,\text{nm}$. The modified unfilled nanoslit N_y has length $l_y = 470\,\text{nm}$ and width $w_y = 83\,\text{nm}$. These values for length and width are obtained from Eqs. (1) and (2) with the design goal of achieving a $\lambda/4$ wave plate. As shown in Fig. 2(b), the modified nanoslits N_x and N_y both have resonance wavelengths of 802 nm. One transmission spectrum is of an unfilled nanoslit for a plane wave illumination polarized perpendicular to the slit. The other transmission spectrum is for a glass-filled nanoslit, again for a plane wave illumination polarized perpendicular to the slit.

Although Fig. 2(b) shows that the resonance wavelengths match, it can be seen that the transmission amplitudes differ due to the different length/width ratios and the nanoslits being filled with different materials.

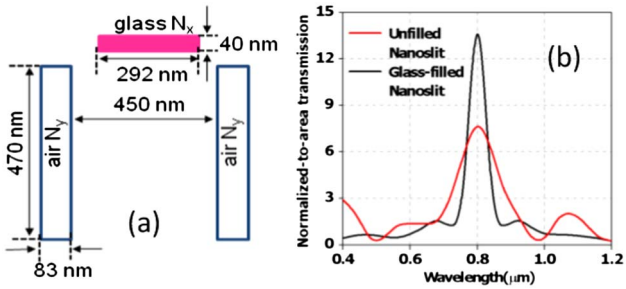

Fig. 2. (Color online) (a) Schematic layout of a device comprising two unfilled nanoslits and a filled nanoslit to produce the same overall transmission amplitude coefficients for the x and y polarizations, but differing in phase by $\pi/2$. (b) Transmission spectrum of an unfilled nanoslit and spectrum of a filled nanoslit. It can be seen that the amplitude transmitted through the unfilled nanoslit is half that of the filled nanoslit.

The transmission for the glass-filled nanoslit is approximately twice as large as that of the unfilled slit. Here, we consider a wave plate for which equal amplitudes are important in order for the linearly polarized input beam to be converted to a circularly polarized output beam. One means of achieving this is for the structure to comprise two unfilled nanoslits and a glass-filled slit, as shown in Fig. 2(a).

To demonstrate its functionality of as a wave plate, we simulate the transmission that results from a linearly polarized plane wave illumination of the structure shown in Fig. 2(a). We plot the amplitudes of the E_x and E_y components of the electric field as a function of distance from the metal–air interface in Fig. 3(a).

It can be seen that E_y lags behind E_x after passing through the nanoslits. This is due to the fact that the E_x fields are transmitted through the N_y nanoslits, while the E_y fields are from the glass N_x nanoslit. The N_x nanoslit has a larger phase delay. From Fig. 3(a), it can be seen that the crests of E_x and E_y are spaced 200 nm apart, which corresponds to $\lambda/4$. Another observation is the decay of the field amplitude as a function of distance along the z-axis due to diffraction from the nanoslits that are of subwavelength dimensions. The inset of Fig. 3(a) shows the total power, found by integrating the longitudinal

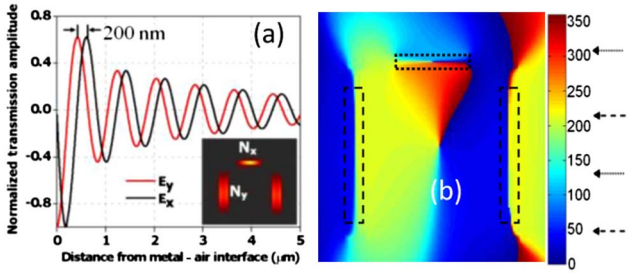

Fig. 3. (Color online) (a) Amplitudes of E_x and E_y components as a function of distance from the metal–air interface. E_y lags behind E_x with a phase difference of $\pi/2$. (Inset) Poynting vector distribution at the metal–air interface. (b) Phase E_z transmitted through nanoslits, showing a phase difference of $\pi/2$ between filled and unfilled slits. The dotted arrows indicate the phases at the top and bottom parts of the glass nanoslit. The dashed arrows indicate the phases on the left and right parts of the unfilled nanoslits. It can also be seen that the pair of arrows associated with each type of slit differ in phase by π rad, indicating resonant transmission.

component of the Poynting vector at the metal–air interface. The power transmitted through the glass-filled nanoslit N_x is twice as large as that of each unfilled nanoslit, in agreement with the transmission simulations of Fig. 2(b). With this result, the objective of designing a $\lambda/4$ plasmonic wave plate based on nanoslits is achieved.

The E_z phase distribution is shown in Fig. 3(b). It can be seen that the phase of E_z in N_x is delayed by $\pi/2$ radians with respect to that in N_y. To facilitate the comparison of phases within the slits, two pairs of arrows phases observed within the nanoslits are marked on the right side of the phase legend. The dotted arrows correspond to the phases within the N_x slit, while the dashed arrows are for the N_y slits. It can be seen that there is a phase difference of $\pi/2$ rad between the nanoslits. It should also be noted that the phase of E_z varies by π across with width of each slit. The device generates a right circularly polarized (RCP) output from the input linear polarization. If the N_x and N_y nanoslits were to be switched to make E_x lag behind E_y, a left circularly polarized (LCP) output would be generated. Besides converting linear to circular polarization, the opposite conversion is also possible, with circularly polarized light being converted to linearly polarized light.

In Fig. 4, the transmitted phase for glass-filled and unfilled nanoslits with lengths of 292 and 470 nm, respectively, are plotted as a function of nanoslit width, as determined by Eqs. (1) and (2). The horizontal lines are drawn to indicate the phases predicted for glass-filled and unfilled slits with widths of 40 and 83 nm, respectively, as shown in Figs. 2 and 3. It can be seen that these are predicted to differ in phase by $\pi/2$ rad, with the E_x field leading the E_y field. The good agreement between the results obtained from the analytical method, i.e., Eqs. (1) and (2), and the FDTD simulations demonstrates the effectiveness of the analytical method. This is advantageous as it implies that through Eqs. (1) and (2), wave plates with a wide range of phase differences can be created without the need to rely on computationally expensive FDTD simulations.

The device we have discussed thus far consists of an isolated group of two or three nanoslits. The input field is a plane wave, but the transmitted field is more akin to the field from a point source. We now consider a means for

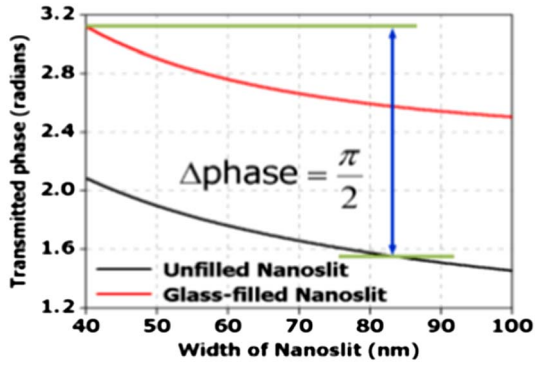

Fig. 4. (Color online) Phase of fields transmitted by unfilled and glass-filled nanoslits versus slit width. The phases predicted for unfilled and glass-filled nanoslits of 83 and 40 nm, respectively, are indicated with horizontal lines. It can be seen that the predicted phase difference of $\pi/2$ matches that found by the FDTD.

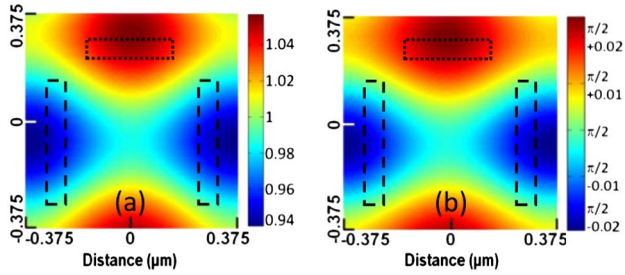

Fig. 5. (Color online) (a) Ratio of $\langle|E_y|\rangle/\langle|E_x|\rangle$ plotted over a unit cell, showing a value of 1 ± 0.06 is achieved. (b) Phase difference between y- and x-polarized transmitted fields plotted over a unit cell. It can be seen that phase(E_y) – phase$(E_x) = \pi/2 \pm 0.03$ rad. The incident wavelength is 802 nm.

achieving a plane wavelike output from the device. This is achieved using a periodic array of nanoslits, with the unit cell comprising the structure of Fig. 2(a). The x and y periods are 750 nm. The amplitude and phase differences in the far-field over a unit cell are shown in Fig. 5. It can be seen that, as required, the amplitude ratio is very close to unity and the phase difference is very close to $\pi/2$.

In conclusion, we propose the realization of $\lambda/4$ wave plates with subwavelength dimensions using nanoslits. The predictions of a semianalytical model for the phase shift are shown to be in good agreement with FDTD simulations. Linearly polarized light can be converted to LCP or RCP, depending on the orientation of the nanoslits. We anticipate that the wave plate we introduce may be advantageous for polarization conversion and detection in nanoscale photonic circuits.

This work was supported (in part) by the Defense Advanced Research Projects Agency (DARPA) N/MEMS S&T Fundamentals program under grant N66001-10-1-4008 issued by the Space and Naval Warfare Systems Center Pacific (SPAWAR).

References

1. T. W. Ebbesen, H. J. Lezec, H. F. Ghaemi, T. Thio, and P. A. Wolff, Nature **391**, 667 (1998).
2. J. A. Porto, F. J. Garcia-Vidal, and J. B. Pendry, Phys. Rev. Lett. **83**, 2845 (1999).
3. F. Yang and J. R. Sambles, Phys. Rev. Lett. **89**, 063901 (2002).
4. L. Novotny and B. Hecht, *Principles of Nano-Optics* (Cambridge University, 2007).
5. Z. Sun and H. K. Kim, Appl. Phys. Lett. **85**, 642 (2004).
6. H. Shi, C. Wang, C. Du, X. Luo, X. Dong, and H. Gao, Opt. Express **13**, 6815 (2005).
7. Z. Marcet, J. W. Paster, D. W. Garr, J. E. Bower, R. A. Cirelli, F. Klemens, W. M. Mansfield, J. F. Miner, C. S. Pai, and H. B. Chan, Opt. Lett. **33**, 1410 (2008).
8. L. Verslegers, P. B. Catrysse, Z. Yu, J. S. White, E. S. Barnard, M. L. Brongersma, and S. Fan, Nano Lett. **9**, 235 (2009).
9. A. Drezet, C. Genet, and T. W. Ebbesen, Phys. Rev. Lett. **101**, 043902 (2008).
10. F. J. G. de Abajo, Opt. Express **10**, 1475 (2002).
11. S. A. Maier, *Plasmonics: Fundamentals and Applications* (Springer, 2007).
12. B. Prade, J. Y. Vinet, and A. Mysyrowicz, Phys. Rev. B **44**, 13556 (1991).
13. E. N. Economu, Phys. Rev. **182**, 539 (1969).
14. F. J. Garcia-Vidal, Esteban Moreno, J. A. Porto, and L. Martin-Moreno, Phys. Rev. Lett. **95**, 103901 (2005).